Modulation of the Ligand–Field Anisotropy in a Series of Ferric Low Spin Cytochrome *c* Mutants derived from *Pseudomonas aeruginosa c*–551 and *Nitrosomonas europaea c*–552. An NMR and EPR Study.

Supporting information

Giorgio Zoppellaro,[‡] *Espen Harbitz,*[‡] *Ravinder Kaur,*[§] *Amy A. Ensign,*[§] *Kara L. Bren*[§*] *and K. Kristoffer Andersson*[‡*]

[‡] Department of Molecular Biosciences, University of Oslo, PO Box 1041 Blindern, Oslo NO–0316, Norway

[§] Department of Chemistry, University of Rochester, Rochester, New York 14627–0216, USA

e-mail: k.k.andersson@imbv.uio.no, bren@chem.rochester.edu

Materials and Methods

EPR spectroscopy and data analyses. The EPR measurements for the wild type forms and mutants of cytochrome *c* from *Pseudomonas aeruginosa* and *Nitrosomonas europaea* (protein concentration 210–310 μM, 50 mM HEPES, pH 7.5) were acquired with a dual–band X–cavity on a Bruker Elexsys 500E spectrophotometer characterized by a cavity quality factor (*Q*) 3800–4000 within the measurements and equipped with a He–flow cryostat (ESR 900, Oxford Instruments). The XSophe (ver. 1.1.3) EPR simulation platform and XeprView (ver. 1.2b.33) software were provided by Bruker.[1] The EPR spectra were baseline corrected upon subtraction of the cavity background and the EPR tube containing buffer (keeping the same filling volume) recorded under identical conditions. The empirical expression used to fit the saturation EPR data follows the work of Portis[2] and Castner[3] as expressed in the following form (eq. 1):

$$\iint I = \frac{k \times \sqrt{P}}{\left[1 + P / P_{1/2}\right]^{b/2}} \qquad (1)$$

Here ∬I describes the double integrated signal intensity, P the applied microwave power, b the relaxation factor ($b = 1$ for inhomogeneous line broadening and $b = 3$ for homogeneous line broadening), $P_{1/2}$ the power at which the signal is half saturated and k an experimental constant associated with the instrument. The value of b depends on which mechanism is dominating the relaxation process of the quanta absorbed. If the spin–lattice relaxation (T_1) represents the dominant factor, the power–dependent line broadening is inhomogeneous (Gaussian–line) and b assumes the minimum value of 1. When T_2 is dominant, the line broadening is homogeneous (Lorentzian–line) and b assumes the maximum value of 3. The relaxation factor b is often allowed to fluctuate in the fitting in order to accounts for intermediate cases ($1 \leq b \leq 3$), when the observed line–shape is a mixture of Lorentzian and Gaussian. In order to apply eq. 1 the following experimental conditions must be satisfied: (i) the samples should be in a region of the cavity with maximum microwave field, thus the filling volume has to be optimized, (ii) the sample temperature must be constant, and (iii) the Zeeman modulation amplitude, the frequency and possibly the gain must also be constant.

Fig. S1. EPR spectra of NeG50N/V65Δ recorded at T = 10 K by (A) slow sample-freezing at –30 °C (ethanol bath, 5 min) and (B) upon annealing. Parameters: (A) 9.66319 GHz frequency, 4 scan and (B) 9.66389 GHz frequency, 4 scan. Then, 100 KHz modulation frequency, 7.46 Gauss modulation amplitude, 82 ms time constant, 168 s sweep time, 0.63 mW microwave power.

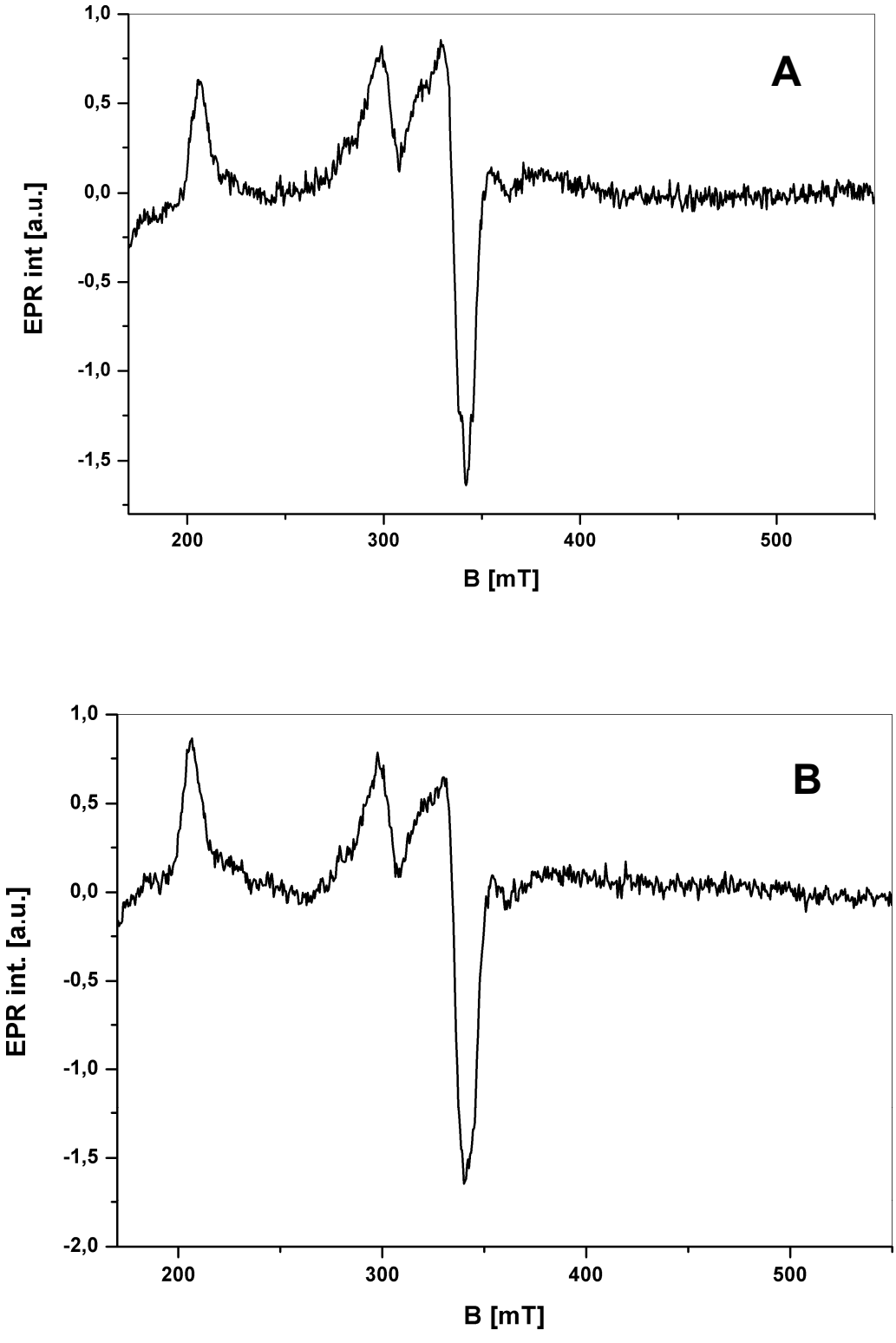

Fig. S2. EPR spectra of NeN64Δ recorded at T = 10 K by (A) slow sample-freezing at –30 °C (ethanol bath, 5 min) and (B) upon annealing. Parameters: (A) 9.66468 GHz frequency, 2 scan and (B) 9.66370 GHz frequency, 2 scan. Then, 100 KHz modulation frequency, 7.46 Gauss modulation amplitude, 82 ms time constant, 168 s sweep time, 1.00 mW microwave power.

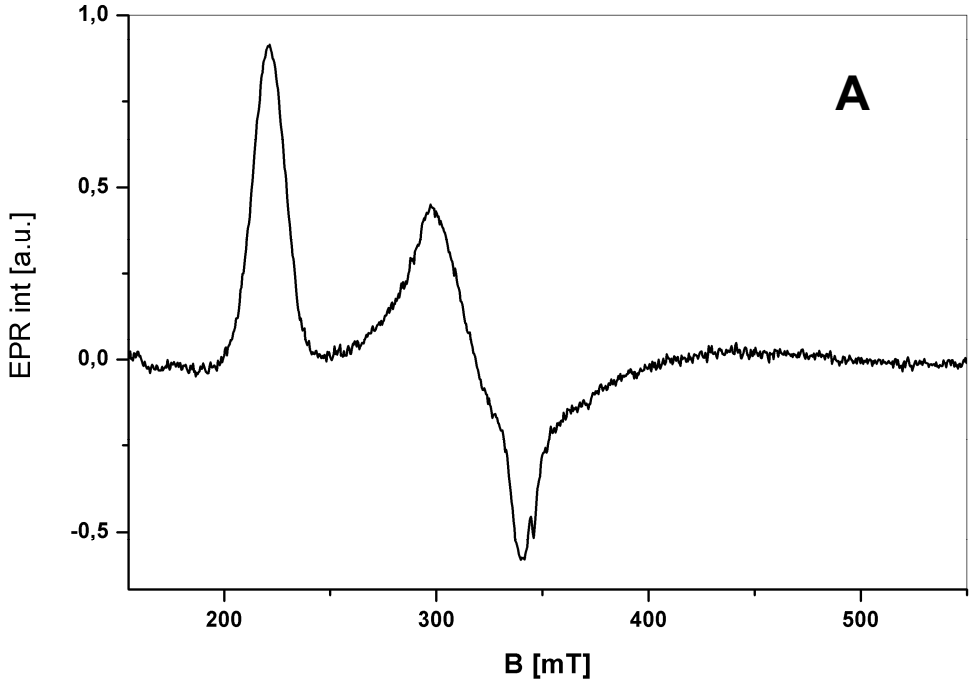

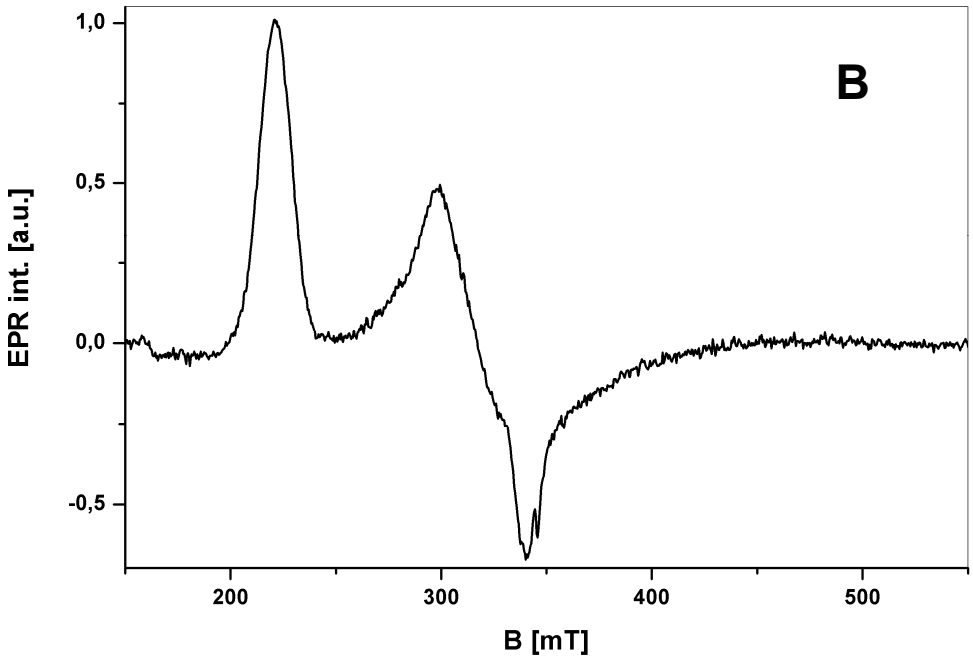

Fig. S3. EPR spectra of PaN64Q recorded at T = 10 K by (A) slow sample freezing at –30 °C (ethanol bath, 5 min) and (B) upon annealing. Parameters: (A) 9.66312 GHz frequency, 2 scan and (B) 9.66375 GHz frequency, 4 scan. Then, 100 KHz modulation frequency, 7.46 Gauss modulation amplitude, 82 ms time constant, 168 s sweep time, 0.8 mW microwave power.

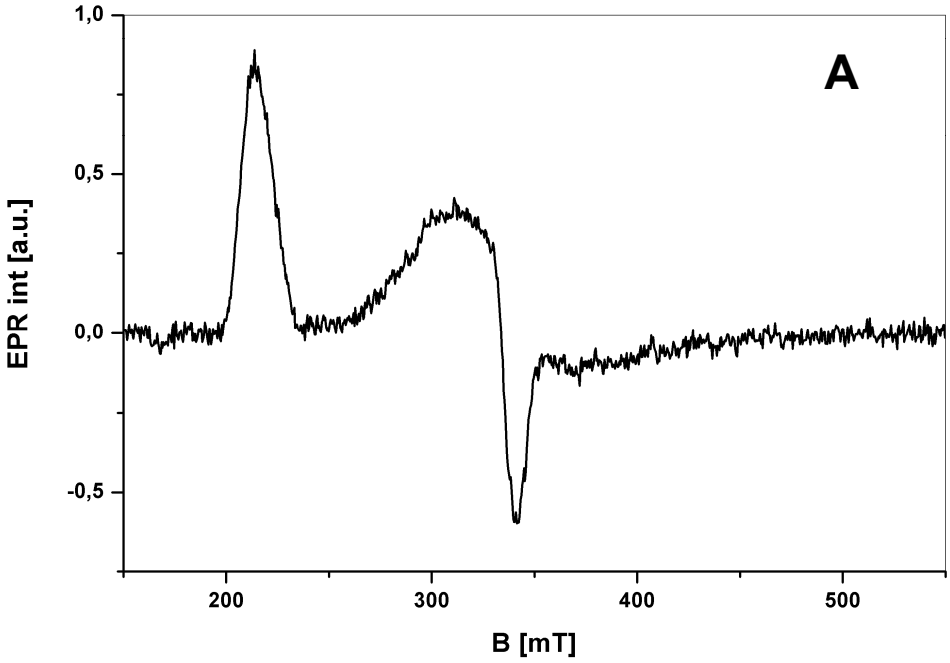

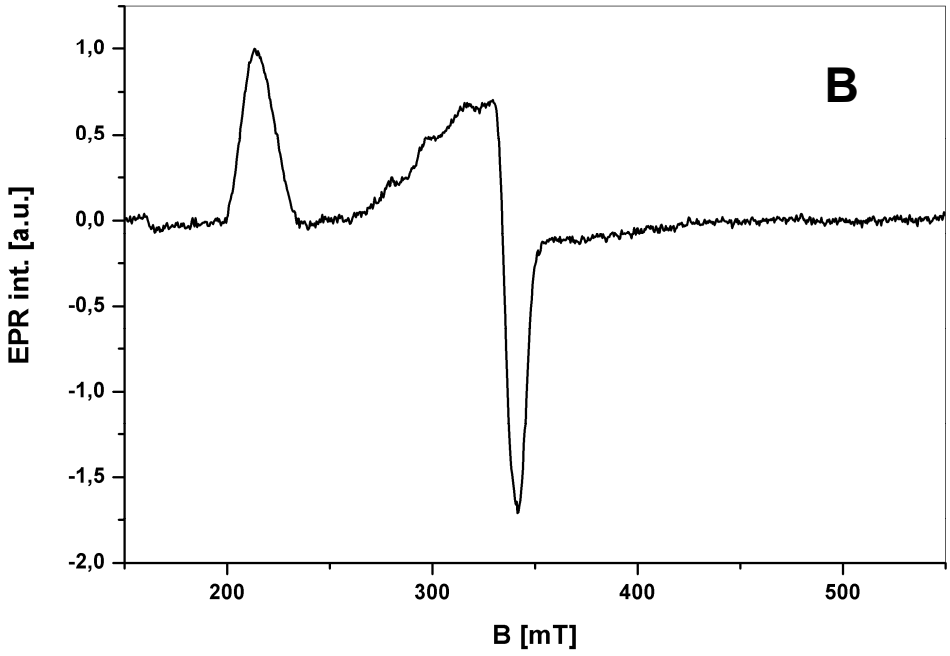

Fig. S4. EPR spectra of NeV65Δ recorded at T = 10 K by (A) slow sample freezing at –30 °C (ethanol bath, 5 min) and (B) upon annealing. Parameters: (A) 9.66751 GHz frequency, 2 scan and (B) 9.66438 GHz frequency, 2 scan. Then, 100 KHz modulation frequency, 7.46 Gauss modulation amplitude, 82 ms time constant, 168 s sweep time, 1.0 mW microwave power.

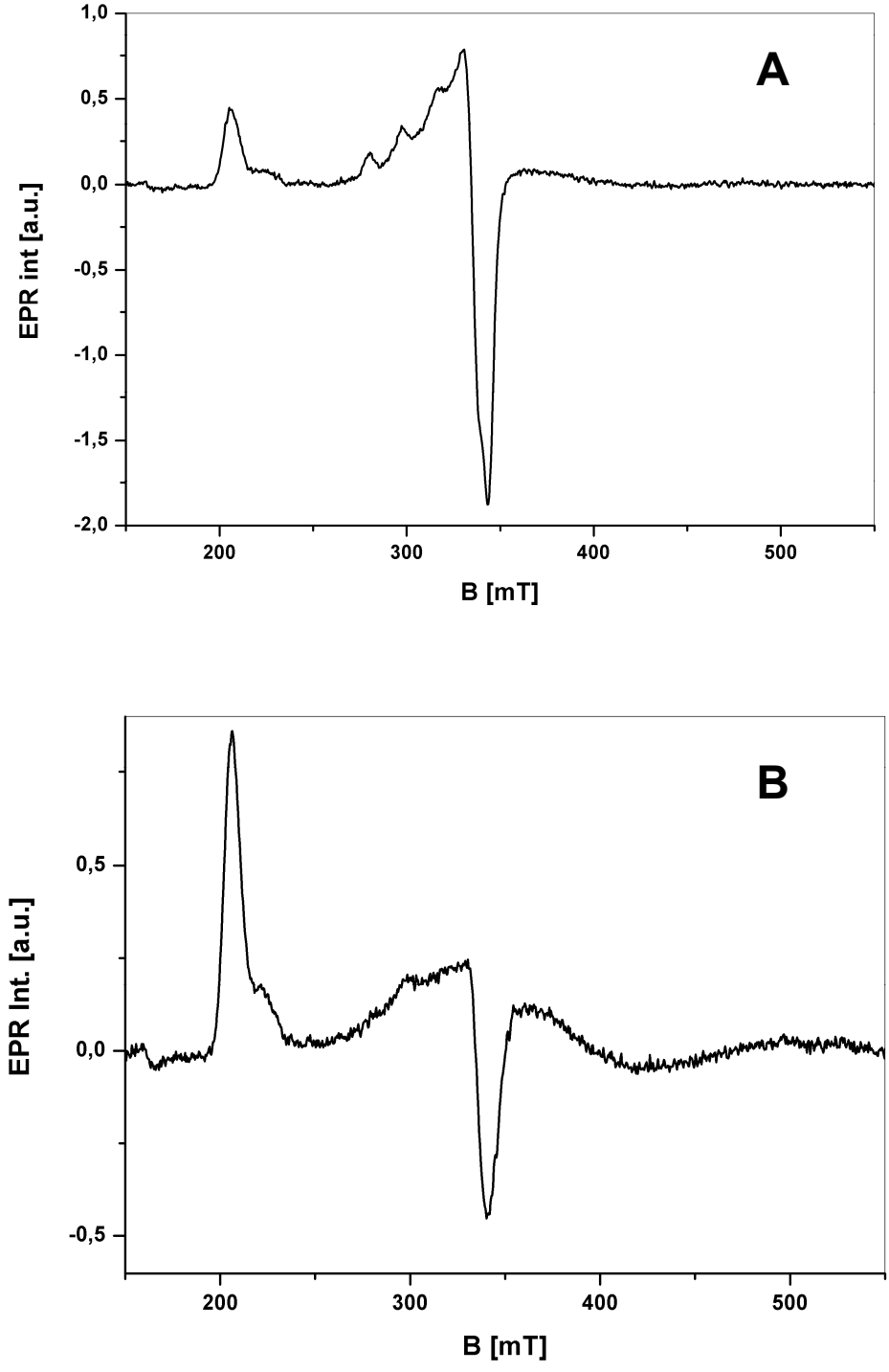

Fig. S5. EPR spectra of PaN50G/V65ins recorded at T = 10 K by (A) slow sample freezing at –30 °C (ethanol bath, 5 min) and (B) upon annealing. Parameters: (A) 9.66277 GHz frequency, 2 scan and (B) 9.66189 GHz frequency, 4 scan. Then, 100 KHz modulation frequency, 7.46 Gauss modulation amplitude, 82 ms time constant, 168 s sweep time, 0.8 mW microwave power.

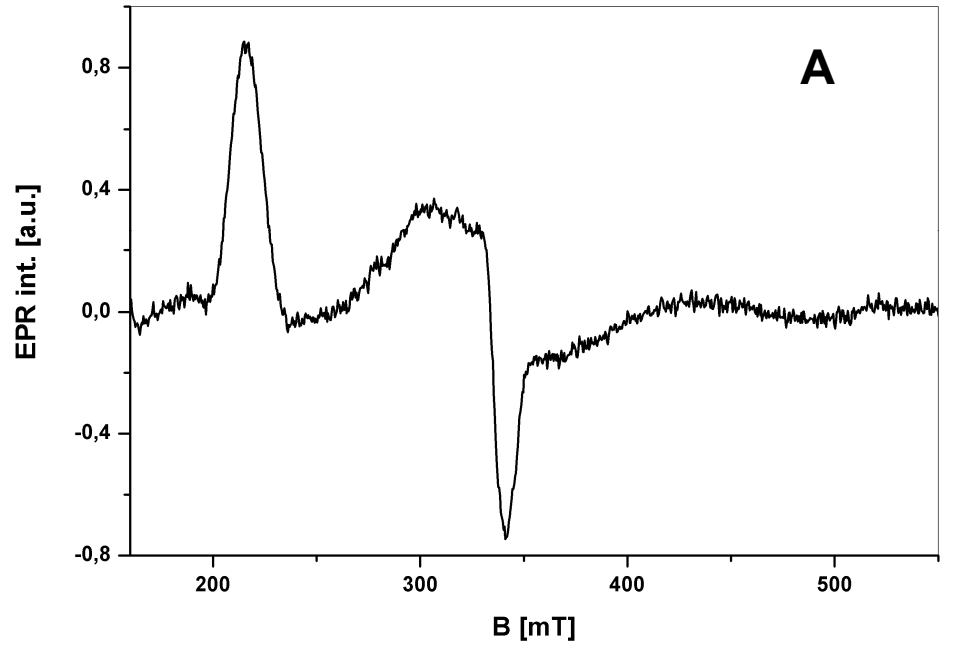

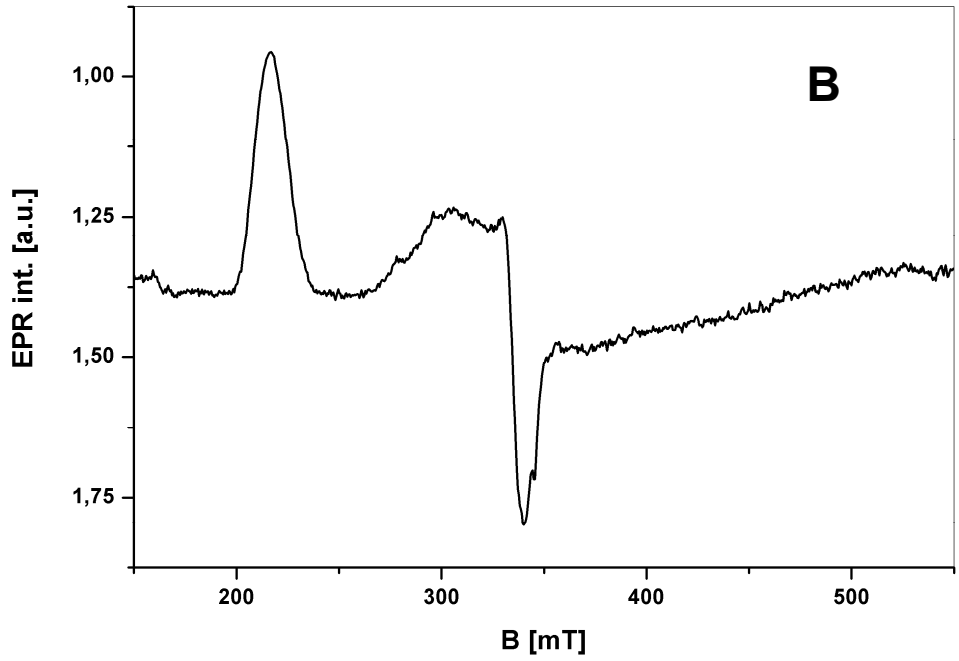

Fig. S6. EPR spectra of PaN64V recorded at T = 10 K by (A) slow sample freezing at –30 °C (ethanol bath, 5 min) and (B) upon annealing. Parameters: (A) 9.66277 GHz frequency, 2 scan and (B) 9.66358 GHz frequency, 2 scan. Then, 100 KHz modulation frequency, 7.46 Gauss modulation amplitude, 82 ms time constant, 168 s sweep time, 1.0 mW microwave power.

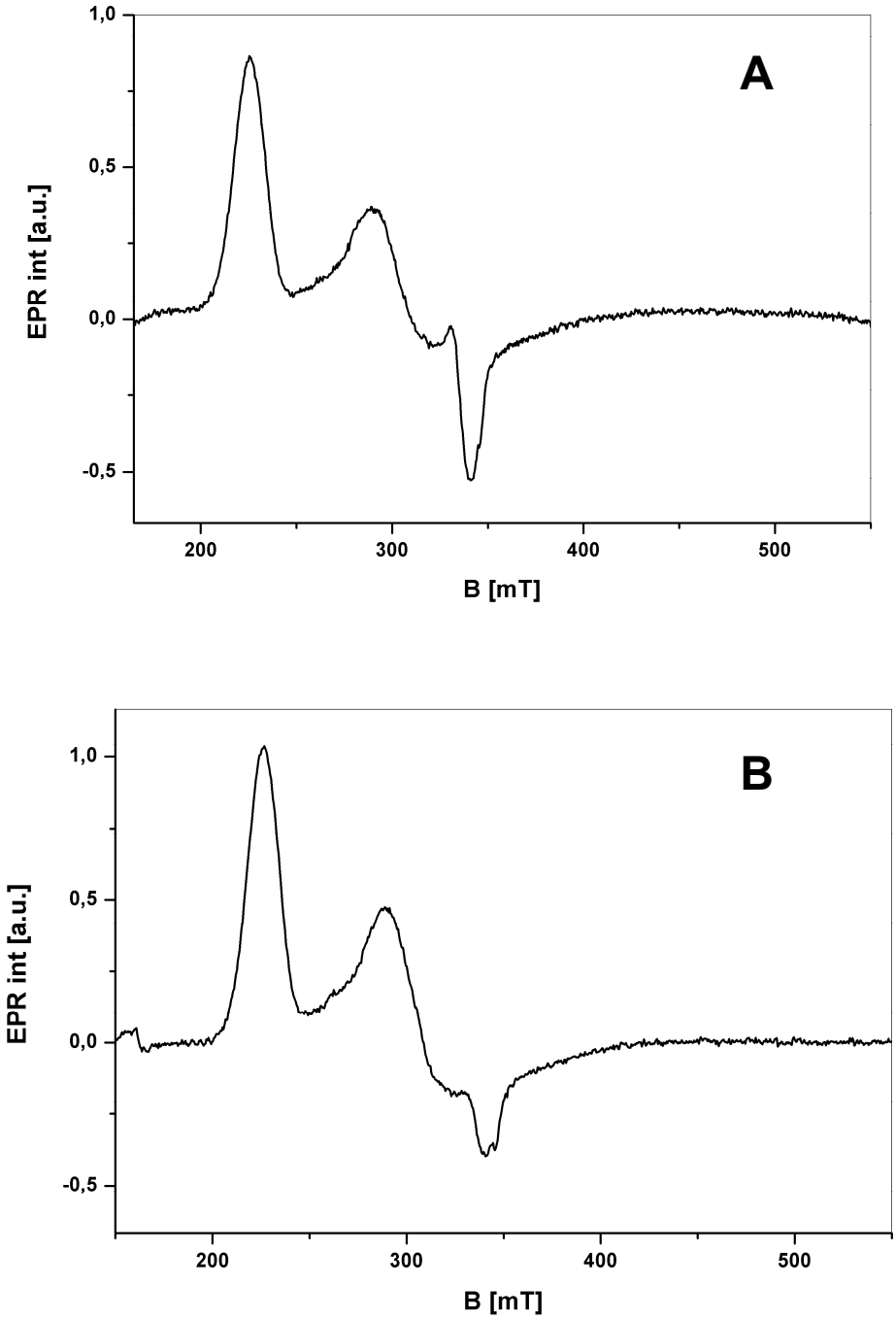

Fig. S7. EPR spectra of Ne *c*-552 recorded at T = 10 K by (A) slow sample-freezing at –30 °C (ethanol bath, 5 min) and (B) upon annealing. Parameters: (A) 9.66359 GHz frequency, 2 scan, 0.63 mW microwave power, and (B) 9.66376 GHz frequency, 2 scan, 0.80 mW microwave power. Then, 100 KHz modulation frequency, 7.46 Gauss modulation amplitude, 82 ms time constant, 168 s sweep time.

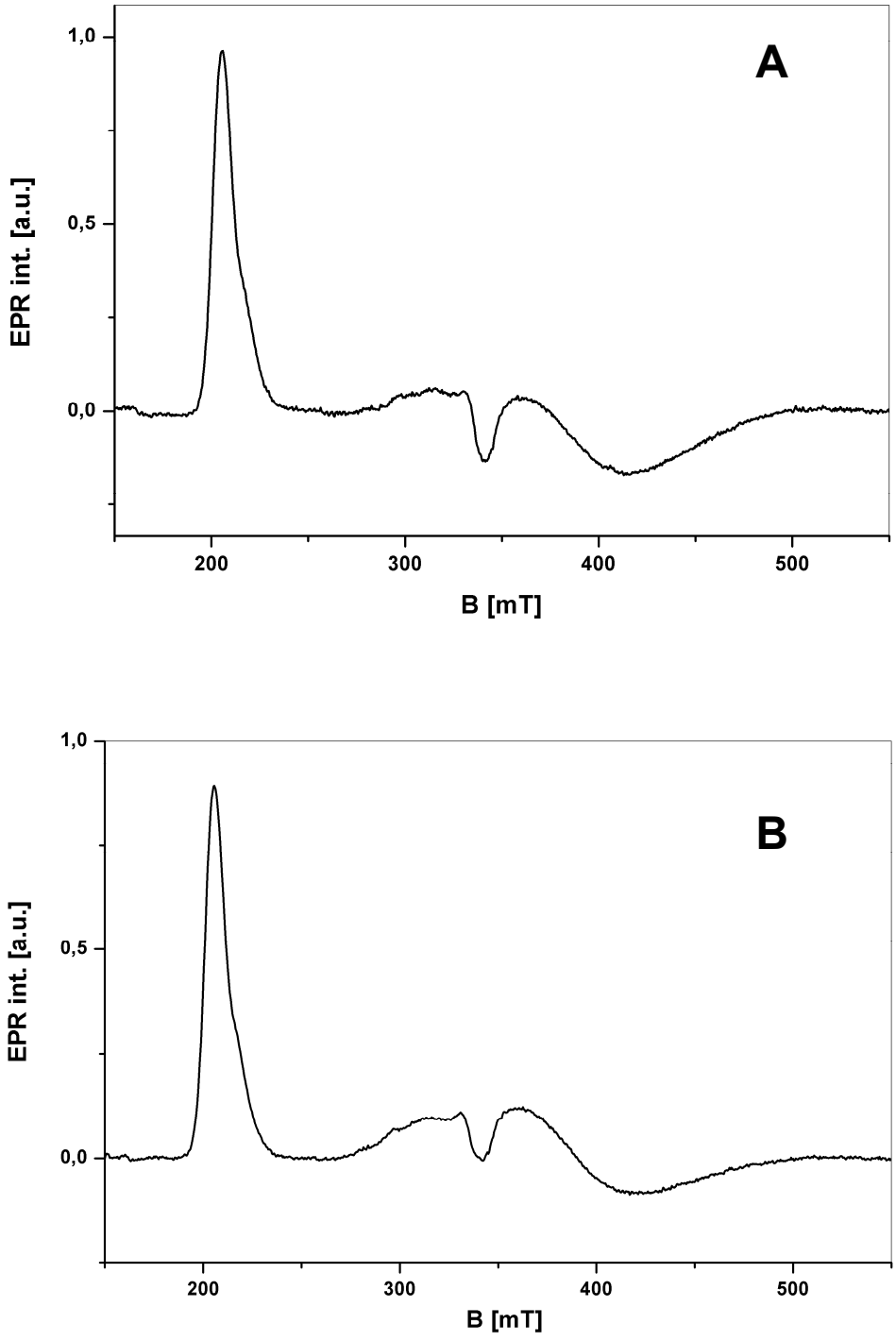

Fig. S8. EPR spectra of Pa *c*-551 recorded at T = 10 K by (A) slow sample-freezing at –30 °C (ethanol bath, 5 min) and (B) upon annealing. Parameters: (A) 9.66823 GHz frequency, 2 scan, 0.80 mW microwave power, and (B) 9.66404 GHz frequency, 2 scan, 0.63 mW microwave power. Then, 100 KHz modulation frequency, 7.46 Gauss modulation amplitude, 82 ms time constant, 168 s sweep time.

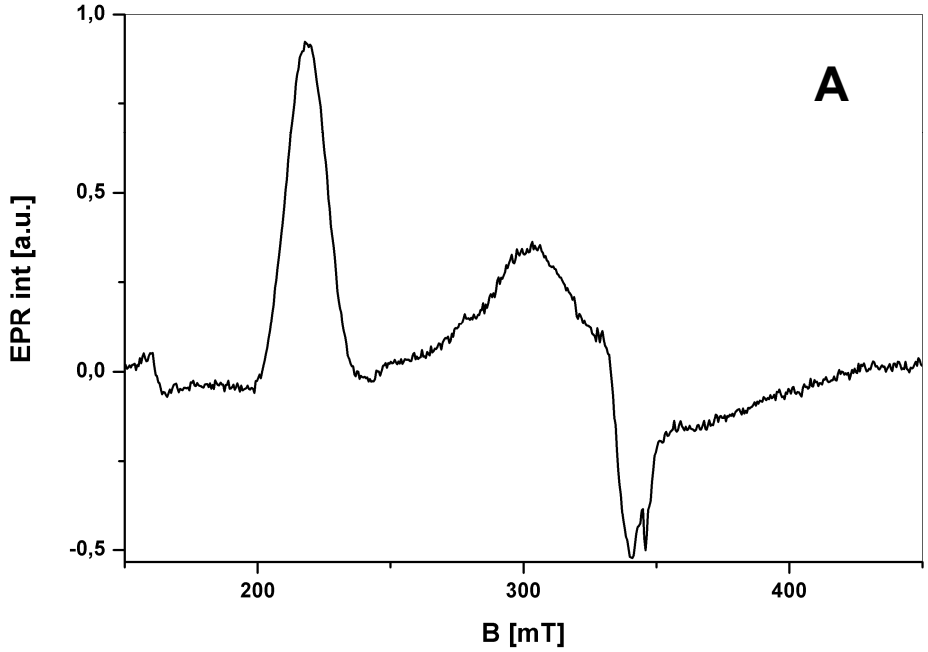

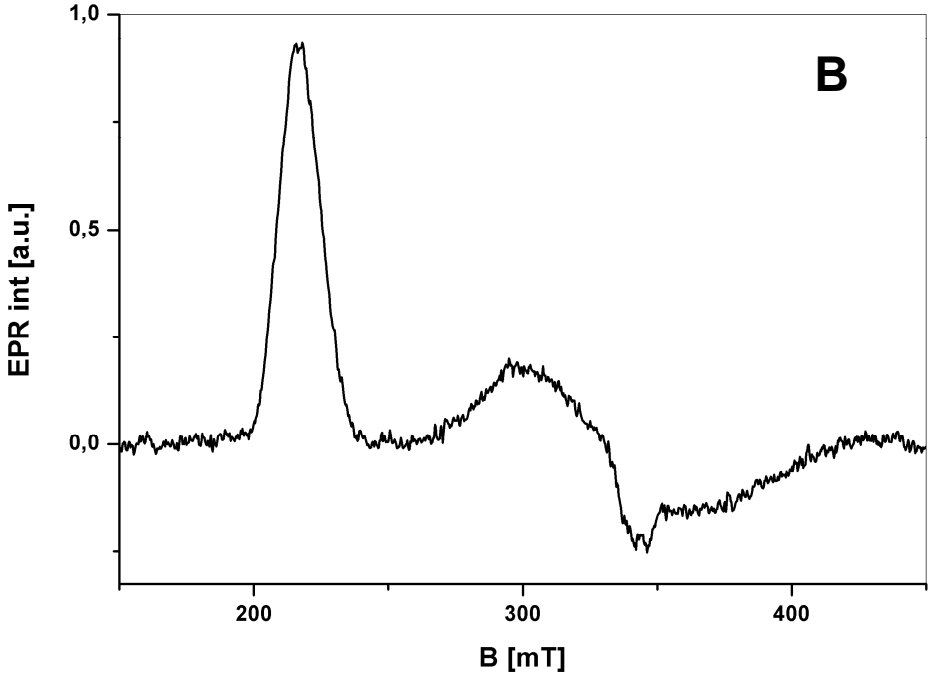

Fig. S9. Correlation between observed g_{max} values *versus* the average heme methyl chemical shift <δ> in the over–expressed Ne *c*–552 and Pa *c*–551 proteins and related mutants with other cytochrome *c*, *b* and *f* type proteins.

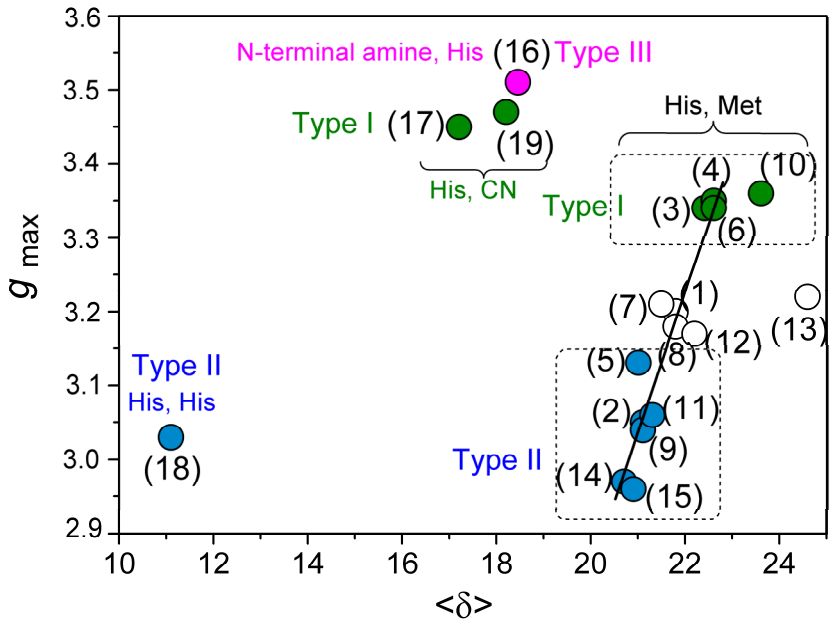

Protein variant	Ref
(1) Pa c-551	[4]
(2) PaN64	[4]
(3) Ne c-552	[5]
(4) NeV65	[4]
(5) NeN64	[4]
(6) NeG50N/V65	[4]
(7) PaN64Q	[4]
(8) PaN50G/V65ins	[4]
(9) Horse cyt c	[6]
(10) B. pasteurii c-553	[5]
(11) Yeast iso-1	[7]
(12) R. rubrum c2	[7]
(13) Rh. palustris c2	[8]
(14) P. ZoBell c-551	[9]
(15) P. stutzeri c-551	[10]
(16) Cyt f	[11]
(17) MetMbCN	[6]
(18) Cyt b5	[6]
(19) Horse Cyt c-CN	[12][13]

REFERENCES

(1) Hanson, G. R.; Gates, K. E.; Noble, J. C.; Griffin, M.; Mitchell, A.; Benson, S. *J. Inorg. Biochem.* **2004**, *98*, 903–916.

(2) Portis, A. M. *Phys. Rev.* **1953**, *91*, 1071–1078.

(3) Castner, T. J. Jr. *Phys. Rev.* **1959**, *115*, 1506–1515.

(4) This work.

(5) Zoppellaro, G.; Teschner, T.; Harbitz, E.; Schünemann, V.; Karlsen, S.; Arciero, D. M.; Ciurli, S.; Trautwein, A. X.; Hooper, A. B.; Andersson, K. K. *Chem. Phys. Chem.* **2006**, *7*, 1258–1267.

(6) Bertini, I.; Luchinat, C.; Parigi, G. *Eur. J. Inorg. Chem.* **2000**, 2473–2480.

(7) Brautigan, D. L.; Feinberg, A. B.; Hoffman, M. B.; Margoliash, E. *J. Biol. Chem.* **1977**, *252*, 574–582.

(8) Bertini, I.; Luchinat, C.; Macinai, R.; Martinuzzi, S.; Pierattelli, R.; Viezzoli, M. S. Inorg. Chim. Acta **1998**, 125–134.

(9) Cheesman, M. R.; Ferguson, S. J.; Moir, J. W. B.; Richardson, D. J.; Zumft, W. G.; Thomson, A. J. Biochemistry **1997**, *36*, 16267–16276.

(10) Van Wonderen, J. H.; Knight, C.; Oganesyan, V. S.; George, S. J.; Zumft, W. G.; Cheesman, M. R. *J. Biol. Chem.* **2007**, *282*, 28207–28215.

(11) Rigby, S. E. J.; Moore, G. R.; Gray, J. C.; Gadsby, P. M. A.; George, S. J.; Thomson, A. J. *Biochem. J.* **1988**, *256*, 571–577.

(12) Gadsby, P. M. A.; Thomson, A. J. *J. Am. Chem. Soc.* **1990**, *112*, 5003–5011.

(13) Shokhirev, N. V.; and Walker, F. A. *J. Biol. Inorg. Chem.* **1998**, *3*, 581–594.